analytical chemistry

Article

pubs.acs.org/ac

Arrayed Profiling of Multiple Glycans on Whole Living Cell Surfaces

Yunlong Chen,[†] Lin Ding,[†] Tingting Liu, and Huangxian Ju*

State Key Laboratory of Analytical Chemistry for Life Science, Department of Chemistry, Nanjing University, Nanjing, Jiangsu 210093, P. R. China

Supporting Information

ABSTRACT: An array-based method for profiling and quantification of multiple glycans on whole living cell surfaces was developed through combining DNA encoding technology with DNA microarray. Using four kinds of lectins as the model to recognize four types of cell surface glycans, the specific barcode-lectin probes that contained the endonuclease cutting site were designed. The barcode-lectin probes had the DNA sequences complementary to four sequences immobilized on a DNA microarray, respectively. After the living cells were incubated with the mixture of four barcode-lectin probes, these probes could bind to cell surface through the specific interaction between the lectins and corresponding glycans. Thus, the glycans and their amounts could be profiled by releasing the barcodes from cell surface with endonuclease cleaving, binding the barcodes to DNA microarray with specific hybridization, and then producing the amplified fluorescence signal with hybridization chain reaction (HCR). The HCR was performed with two kinds of Cy5 labeled hairpins. The average amount of mannose, *N*-acetylgalactosamine, *N*-acetylglucosamine, and *N*-acetylneuraminic acid on BGC cell was obtained to be 6.8×10^7, 3.8×10^7, 2.1×10^8, and 1.1×10^7 moieties per cell, respectively. The proposed method possessed whole cell surface accessibility, powerful distinguishing capability, fast recognition kinetics, easy miniaturization, and high throughput without need of cell pretreatment or labeling. It could become a powerful tool for elucidation of the complex glycan-related biological processes.

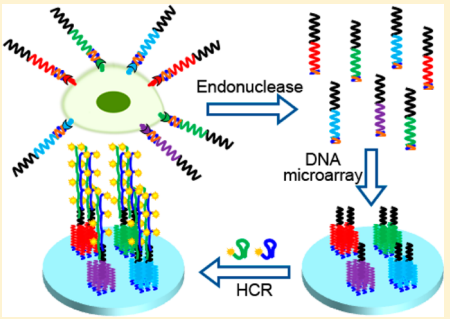

Glycans, composed of ten types of common monosaccharide units, decorate all mammalian cell surfaces.[1] These glycans mediate a wide variety of biological processes, including cell growth and differentiation, cell−cell communication, immune response, pathogen interaction, and intracellular signaling events.[2,3] The structure complexity and microheterogeneity of glycans on living cells depend on their biosynthetic pathway occurring in the endoplasmic reticulum−Golgi[4] and can dynamically reflect the physiological and pathological states of cells.[5−8] More importantly, tumor cells aberrantly express distinct sets of glycans; thus, the glycans can indicate different tumor onset and progression processes.[9] Therefore, simultaneous analysis of multiple glycans on living cell surface may contribute to correlation of the specific glycan patterns with disease states for clinic diagnosis and understanding of their roles in disease development.

Traditional mass spectrometric (MS) analysis of cell surface glycans can provide multiple molecule-level information[10] but requires cell lysis, enzymatic cleavage, and derivatization. It is unsuitable for in situ detection and suffers from the undervaluation of certain glycan groups owing to the limited number of site-specific enzymes and their loss in the corresponding separation process.[11] As an alternative, an encoding-based lectin array technique has been developed for multiplexed glycan profiling.[12−14] However, the immobilization of proteins on microarray surface often leads to the denaturation or inactivation due to their chemical modification and the disproportionately large surface area of the small protein spot,[15] and the high density of protein molecules also results in inaccessibility to the active sites.[16] Moreover, these reported array methods rely on the oversimplified comparison of cell binding extents on different lectin spots and thus fail to provide quantitative information of glycan expression. In addition, owing to the spatial nonuniformity of cell membrane and the comprehensive factors influencing the binding extent, e.g., glycan amount, lectin avidity, and binding multivalency, the use of cell binding extent to represent glycan amount on the whole cell surface brings certain deviation. To obtain quantitative, multiple, and whole-surface glycan expression information on living cells, this work designed several specific barcode-lectin probes with DNA barcoding technology and used these probes to propose a novel solution encoding strategy for in situ analysis of cell surface glycans.

Generally, the molecular encoding technology can be divided into two broad classes: planar arrays (positional encoding) and suspension arrays (solution encoding).[17] The suspension arrays use functionalized particles to recognize the multiple targets and can be performed with biological,[17,18] spectrometric,[19] graphical,[20] electronic,[21] and physical[22] encoding schemes. As an interesting biological scheme, the DNA barcoding technique makes use of the sequence diversity of DNA for identification of different targets.[23−25] Its advantages lie in the abundant

Received: October 1, 2013
Accepted: October 15, 2013
Published: October 15, 2013

   dx.doi.org/10.1021/ac403150n | *Anal. Chem.* 2013, 85, 11153−11158

barcodes achievable and the facile interface with various DNA detection techniques. Here, the DNA barcodes were used to encode lectins for in situ profiling of whole-surface glycans (Scheme 1). They were assembled by hybridization of a linking DNA with a coding DNA and composed of three functional components: (1) double-strand DNA endonuclease cutting site, (2) encoding sequence, and (3) single-strand DNA as the primer of hybridization chain reaction (HCR) (Scheme 1a). The unique encoding sequence was used for certain lectin to specifically bind cell surface glycan. The encoding sequence as well as the HCR primer could be separated from the lectin-bound cells by DNA endonuclease cleaving and was subsequently captured by a DNA microarray to achieve discrimination with HCR (Scheme 1b). The microarray was prepared by immobilizing different sequences on different spots to capture corresponding encoding sequences. The HCR process provided the captured encoding sequences with amplified fluorescence signals, which relied on both cell amount and the expression extent of corresponding cell surface glycans. The proposed glycan profiling method possessed whole-surface accessibility, good resolution, enhanced sensitivity, high throughput, and the advantages of miniaturization and parallelization.

Scheme 1. Schematic Illustration of (a) Barcode-Lectin Probe Preparation and (b) Assay Procedure

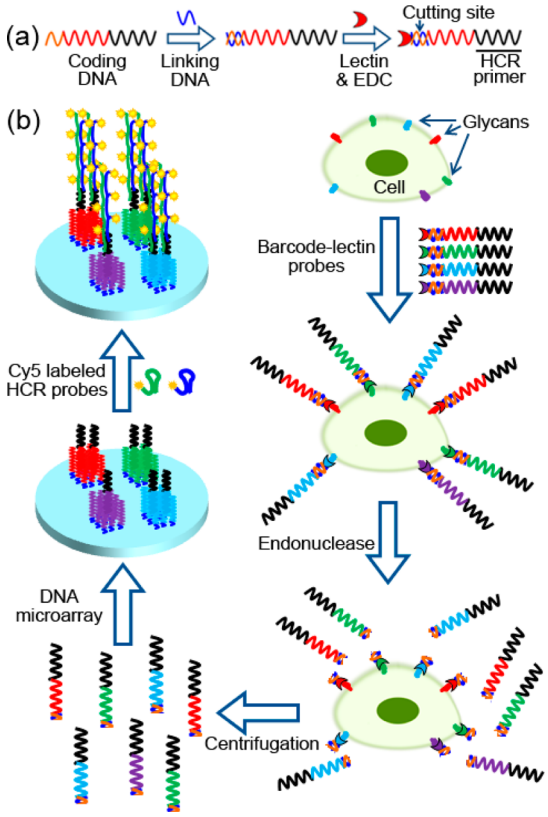

EXPERIMENTAL SECTION

Materials and Reagents. 1-Ethyl-3-(3-dimethylaminopropyl) carbodiimide (EDC), mannose (Man), *N*-acetylgalactosamine (GalNAc), *N*-acetylneuraminic acid (Sia), and *N*-acetylglucosamine (GlcNAc) were purchased from Sigma-Aldrich Inc. (USA). Aldehyde-coated glass slides, print buffer, and hybridization buffer were obtained from Shanghai BaiO Technology Co., Ltd. (Shanghai, China). All lectins and fluorescein labeled lectins, including *Lens culinaris* agglutinin (LCA), fluorescein *Lens culinaris* agglutinin, soybean agglutinin (SBA), fluorescein soybean agglutinin, *Sambucus nigra* agglutinin (SNA), fluorescein *Sambucus nigra* agglutinin, wheat germ agglutinin (WGA), and fluorescein wheat germ agglutinin, were purchased from Vector Laboratories (USA). DNA restriction endonuclease FastDigest DraI was purchased from Thermo (USA). MTT assay kit was purchased from KeyGEN Biotech Co., Ltd. (Nanjing, China). Phosphate buffer saline (PBS, pH 7.4) contained 136.7 mM NaCl, 2.7 mM KCl, 8.72 mM Na_2HPO_4, and 1.41 mM KH_2PO_4. For the lectin–carbohydrate interaction, 0.1 mM $CaCl_2$ and 0.1 mM $MnCl_2$ were added in PBS. All oligonucleotides, including linking DNA (L), four coding DNA (A1, B1, C1, D1), four capturing DNA (A2, B2, C2, D2), and two Cy5-labeled hairpins for HCR (H1, H2) with the sequence listed in Table S1 (Supporting Information), were purchased from Sangon Biological Engineering Technology & Co. Ltd. (Shanghai, China). These sequences were designed to exhibit minimal cross-hybridization. Tris-EDTA (TE) buffer containing 10 mM Tris–HCl and 1 mM EDTA (pH 8.0) was used as DNA stock solution. The HCR buffer was prepared by mixing hybridization buffer and TE buffer (10 mM, pH 8.0) containing 100 mM NaCl and 10 mM $MgCl_2$ (1:1). All aqueous solutions were prepared using ultrapure water (≥18 MΩ, Milli-Q, Millipore).

Apparatus. The microarray was spotted with a Biodot AD1500 biochip production system (Biodot, USA) and scanned with the Biochip Analysis System (Capitalbio, China). The UV–vis absorption spectra were recorded on a Nanodrop-2000C UV–vis spectrophotometer (Thermo, USA). The cell images were obtained with a TCS SP5 laser scanning confocal microscope (Leica, Germany). The MTT assay was performed using 14 Hitachi/Roche System Cobas 6000 (Tokyo, Japan) at 550 nm. Flow cytometric analysis was performed on a Cytomics FC500 flow cytometer (Beckman-Coulter, USA).

Cell Culture and Treatment. BGC-823 cells were purchased from KeyGEN Biotech Co., Ltd. (Nanjing, China) and cultured in RPMI 1640 medium (GIBCO) supplemented with 10% fetal calf serum (FCS, Sigma), penicillin (100 μg mL^{-1}), and streptomycin (100 μg mL^{-1}) at 37 °C in a humidified atmosphere containing 5% CO_2. The cell cycle period and the interphase of BGC-823 cells were 41 and 40 h, respectively. At the logarithmic growth phase, the cells were trypsinized and washed twice with culture medium by centrifugation at 1000 rpm for 3 min. The sediment was resuspended in the culture medium to obtain a homogeneous cell suspension. Cell number was determined using a Petroff-Hausser cell counter (USA).

Preparation of Capturing DNA Microarray. All capturing DNA solutions were prepared in 1:1 mixed TE buffer and print buffer with a final concentration of 2 μM and then spotted to aldehyde coated glass slides at 50% humidity and room temperature. Each slide contained 48 identical subarrays (4 × 12), and each subarray was constituted by 20 spots (5 × 4) with 5 replicate spots for each capturing DNA. The diameter of DNA spots was about 100 nm. After reaction overnight, the slides were washed with water thrice and dried with nitrogen stream. To block the unreacted aldehyde group, the slides were subjected to incubation with 50 μM of

dx.doi.org/10.1021/ac403150n | *Anal. Chem.* 2013, 85, 11153–11158

ethanolamine solution in TE buffer for 1 h. The slides were then washed with water thrice and dried with nitrogen stream.

Preparation of Barcode-Lectin Probes. 1.0 μM linking DNA was first mixed with 1.0 μM of different coding DNA sequences in PBS buffer at 37 °C in a thermostat shaker and incubated for 2 h, respectively. 0.5 μM of the corresponding lectin and 1 mg/mL EDC solution were then added to the mixture. After reaction for 4 h at 37 °C in a thermostat shaker, the mixture was purified to remove unreacted DNA using a centrifugal filter unit (50 kD) at 5000 rpm for 5 min thrice. The obtained barcode-lectin probe was dispersed in PBS buffer at a final concentration of 0.5 μM.

Profiling of Cell Surface Glycans. BGC-823 cells were incubated with the mixture of 0.1 μM barcode-lectin probes for 1 h at room temperature. After washing by centrifugation at 1000 rpm for 3 min thrice, the probe-bound cells were incubated with 50 U/mL DNA restriction endonuclease in 1X Fastdigest buffer at 37 °C in a thermostat shaker for 15 min. After the mixture was centrifuged at 2000 rpm for 3 min, the supernatant was collected for analysis of the released DNA with a capturing DNA microarray.

The DNA analysis was carried out by dropping a 10 μL mixture of the supernatant or DNA solution and hybridization buffer (1:1) onto a capturing DNA microarray to react for 90 min at 37 °C and then performing the HCR after the array was washed with water thrice and dried with nitrogen stream. The HCR was performed by dropping 10 μL of 2 μM H1 and H2 hairpins in HCR buffer to react at 37 °C for 30 min. After the array was washed with water thrice and dried with nitrogen stream, the fluorescence signal was measured with a biochip analysis system. Pseudocolor images of the microarrays with each color mapped to a certain fluorescence intensity were automatically obtained. The mean color scale intensity (I) of each spot was also recorded to represent fluorescence intensity for data processing, varying from 0 for black to 65 536 for white.

Monosaccharide Inhibition Assay. The mixture of 0.1 μM barcode-lectin probes was incubated with 100 μM Man, GalNAc, Sia, and GlcNAc for 1 h at room temperature, respectively, to obtain corresponding monosaccharide-inhibited samples. The samples were purified using a centrifugal filter unit (50 kD) at 5000 rpm for 5 min thrice, respectively, and then dispersed in PBS for performing the profiling experiment of cell surface glycans using 1×10^5 cells/mL BGC cells.

Flow Cytometric Analysis of Glycan Expression on BGC Cells. BGC cells were collected and suspended in cold PBS buffer. 0.1 μM fluorescein lectin was mixed with 1 mL of 1×10^6 cells/mL cell suspension. After incubation for 60 min, the cells were washed by centrifugation at 1000 rpm for 3 min twice, resuspended in 1 mL PBS, and assayed by flow cytometry. The BGC cells without any treatment were used as the negative control for estimation of autofluorescence.

RESULTS AND DISCUSSION

Characterization of Barcode-Lectin Probes. For proof-of-concept, four types of lectins, which exhibit different glycan binding preferences as listed in Table 1, were used. As shown in Scheme 1a, four barcode-lectin probes were first assembled using different coding DNA (A1, B1, C1, D1) to correspond to different lectins. The linking DNA was first hybridized with coding DNA to form a double-stranded barcode with endonuclease cutting site (X-L, X represented A1, B1, C1, or D1). The carboxyl group at 5′ end of linking DNA was then

Table 1. Glycan-Binding Specificity[a] of Lectins Used in This Work

lectin	source	binding specificity[b]	coding DNA
LCA	*Lens culinaris* (lentil) seeds	αMan, αGlc	A1
SBA	*Glycine max* (soybean) seeds	α>βGalNAc	B1
SNA	*Sambucus nigra* (Elderberry) bark	Siaα6Gal/GalNAc	C1
WGA	*Triticum vulgaris* (wheat germ)	GlcNAc	D1

[a]Ref: Vector Laboratories Web site (http://www.vectorlabs.com/data/protocols/K4−K7.pdf). [b]Glc and Gal represent glucose and galactose, respectively.

conjugated to lectin through EDC-mediated carbodiimide chemistry to obtain barcode-lectin probe (X-L-lectin). For characterization of the linkage, the UV−vis spectra of four groups of lectins, coding DNA and barcode-lectin probes, were shown in Figure S1, Supporting Information. The coding DNA showed the characteristic absorption peaks of oligonucleotides around 260 nm, while lectins exhibited the absorption peaks of proteins around 280 nm. The superimposed peaks of barcode-lectin probes confirmed that lectins were bound to the barcodes successfully via linking DNA. The barcode-lectin probes integrated the recognition specificity of lectins to cell surface glycans and DNA sequences for discrimination.

Performance of DNA Microarray. DNA microarray is a low-cost, high-throughput, and miniaturized technology and has become a powerful tool for large-scale genomic analysis.[26−28] Corresponding to four barcode-lectin probes, four types of capturing DNA (A2, B2, C2, D2) were printed on different spots of an aldehyde-coated glass slide. Ethanolamine was employed to block the glass slide for reducing nonspecific adsorption. Five replicates for each capturing DNA provided efficient quality control of the array. Owing to the small size of the array spot and the small amount of target presented, the signals of DNA array were amplified with HCR prior to data collection by imaging devices. The HCR with Cy5-labeled hairpins H1 and H2[29] produced a long double-strand DNA with the amplified fluorescence signal readout.

The one-to-one hybridization between coding DNA and capturing DNA was first demonstrated by dropping individual coding DNA on DNA microarray (Figure 1). Only the spot of

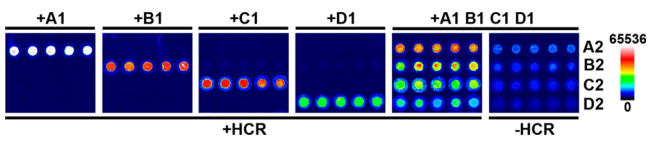

Figure 1. Images of capturing DNA microarray after incubation with 10 nM A1, B1, C1, or D1 or the mixture of 2.5 nM A1, B1, C1, and D1 followed by HCR and without HCR.

corresponding capturing DNA showed obvious fluorescence after HCR, while almost indiscernible signal occurred on other spots, suggesting the specific hybridization between the designed DNA pairs with negligible cross interference. These results allowed the simultaneous detection of multiple coding DNA (A1, B1, C1, D1, Figure 1). The signal difference among different coding DNA sequences at the same concentration could be attributed to their different melting temperatures. This phenomenon would not interfere with subsequent glycan detection, because the real released DNA amount could be calibrated using the standard curves of DNA microarray. The

dx.doi.org/10.1021/ac403150n | Anal. Chem. 2013, 85, 11153−11158

signal amplification capability of HCR was also demonstrated by comparing the fluorescence signals with and without addition of H2 hairpin (Figure 1). In the absence of H2 hairpin, only H1 hairpin was bound to the coding DNA, while the HCR was triggered in the presence of both H1 and H2 hairpins. The A2, B2, C2, and D2 spots after HCR showed 14.4, 13.3, 10.9, and 8.2 times greater signals than those without HCR, respectively.

In order to quantify the released DNA, the array image and standard curves for detection of coding DNA were obtained with the DNA microarray (Figure 2). With the increasing

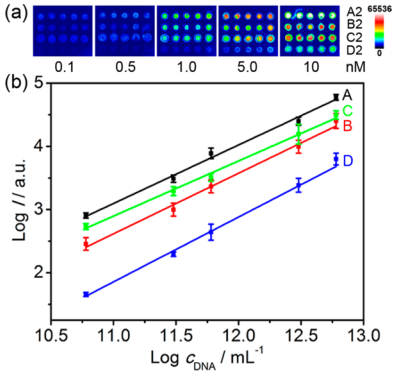

Figure 2. (a) Images of capturing DNA microarray after incubation with the mixture of 0.1, 0.5, 1.0, 5.0, and 10 nM A1, B1, C1, and D1 followed by HCR and (b) plots of logarithm of I vs logarithm of coding DNA concentration for A1, B1, C1, and D1 (from A to D).

concentration of coding DNA (m), all the signals (I) for four coding DNA sequences became greater (Figure 2a). In the concentration range from 6×10^{10} to 6×10^{12} copies/mL, they followed the eq 1 with the R values of 0.996, 0.991, 0.994, and 0.992 for A1, B1, C1, and D1, respectively (Figure 2b). The corresponding slope a and intercept b_1 were 0.926 and −7.09, 0.959 and −7.93, 0.872 and −6.70, 1.026 and −9.43, respectively.

$$\log(I) = a \times \log(m) + b_1 \quad (1)$$

Probe Recognition and Release. The barcode-lectin probes could specifically recognize different cell surface glycans to translate glycan information to barcodes. In order to demonstrate the role of lectins, control cells and the cells incubated with barcode (A1-L) or barcode-lectin probe (A1-L-LCA) were observed after the HCR procedure with laser scanning confocal microscopy, respectively (Figure 3). The cells incubated with the barcode-lectin probe showed an obvious fluorescence signal of Cy5 (Figure 3c), while the cells incubated with A1-L showed a weak signal due to the nonspecific adsorption of A1-L on the cell surface (Figure 3b), verifying the lectin-mediated recognition of the probe on the cell surface. Due to the low cell surface HCR efficiency in physiological buffer, the fluorescence signal was relatively weak.

To decode the barcodes by a DNA microarray, the barcodes were released from cell surface with an endonuclease treatment by designing a DNA endonuclease cutting site in the barcode structure (Scheme 1a). After endonuclease treatment and HCR procedure, the probe-bound cells showed much weaker fluorecence compared to that without endonuclease treatment (Figure 3d), demonstrating the endonuclease cleaving effect.

The lectin-mediated binding was also examined using a capturing DNA microarray. After the living cells were,

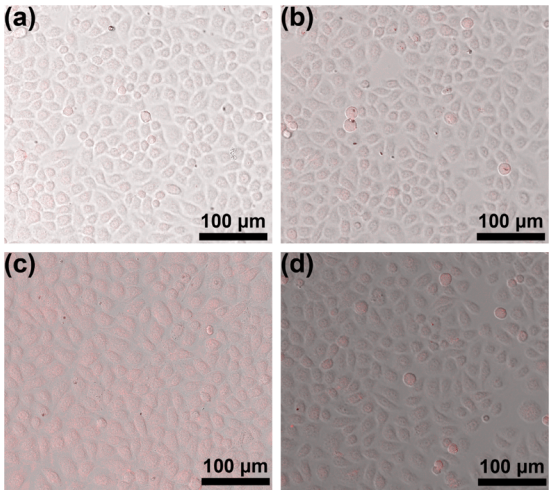

Figure 3. Confocal fluorescence and bright-field overlapped images of (a) control, (b) A1-L treated, (c) A1-L-LCA treated, and (d) A1-L-LCA and then endonuclease treated cells followed with HCR.

respectively, incubated with buffer (control) and the mixture of four barcodes or barcode-lectin probes, they were subjected to the same cleaving, supernatant collection, capturing, and HCR steps. The supernatants of control and barcode-treated cells did not show any signal on the DNA microarray (Figure 4a,b). Contrarily, the supernatant of probe-incubated cells

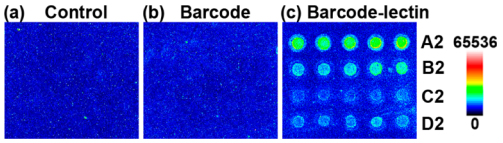

Figure 4. Images of capturing DNA microarray after incubation with DNA released from (a) control cells, (b) cells treated with the mixture of four barcodes, and (c) cells treated with the mixture of four barcode-lectin probes followed with HCR.

displayed obviously signal (Figure 4c) with intensity difference among different capturing DNA, demonstrating the successful release of the barcodes from cell surface and the capture by DNA microarray. Using A1 and LCA as the model, the cells did not show obvious viability change after they were incubated with A1, L, A1-L, and A1-L-LCA probe, while endonuclease treatment resulted in little decrease of cell viability, which would not change the amount of released DNA (Figure S2, Supporting Information), suggesting the feasibility of the probes to profile cell surface glycans.

Recognition Specificity. The specific recognition of barcode-lectin probes to corresponding cell surface glycans was also verified by the monosaccharide inhibition test. After the barcode-lectin probes were, respectively, preincubated with Man, GalNAc, Sia, and GlcNAc, they were subjected to cell incubation, endonuclease treatment, microarray capturing, and HCR with the same operation procedures. Each monosaccharide could notably inhibit the binding of the corresponding probe to cell surface (Figure 5a). The inhibition efficiency, defined as signal decrease percentage, of Man, GalNAc, Sia, and GlcNAc to their probes was calculated to be 88.2%, 83.4%, 83.4%, and 85.0%, respectively (Figure 5b). The inhibition of monosaccharide to other probes was imperceptible, suggesting negligible cross-interference among four recognition pairs,

dx.doi.org/10.1021/ac403150n | Anal. Chem. 2013, 85, 11153−11158

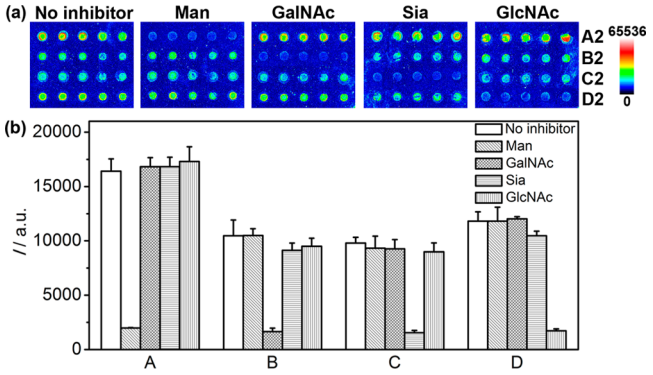

Figure 5. (a) Images of capturing DNA microarray and (b) average spot intensity for the monosaccharide inhibition test using the mixture of four probes in absence of inhibitor and presence of Man, GalNAc, Sia, and GlcNAc, respectively. A, B, C, and D correspond to capturing DNA A2, B2, C2, and D2.

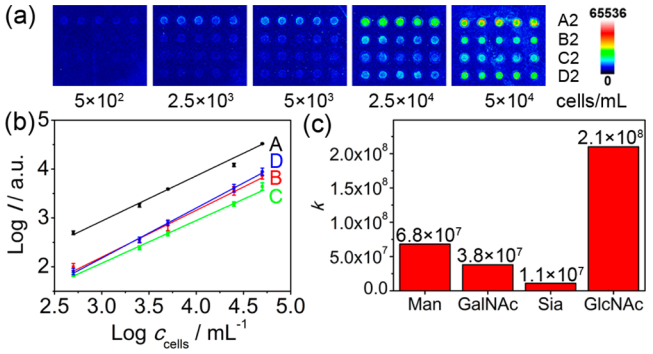

Figure 6. (a) Capturing DNA microarray images after incubation with DNA released from barcode-lectin probe treated cells of different concentrations followed with HCR, (b) plots of logarithm of I vs logarithm of cell concentration for A1-, B1-, C1-, and D1-contained probes (from A to D), and (c) average amounts of surface glycans on each cell.

which verified the recognition specificity of each barcode-lectin probe.

Quantitative Detection of Multiple Cell Surface Glycans. In order to obviate the interference of unbound probe, the cell suspension should be carefully rinsed for three times by centrifugation after incubated with barcode-lectin probes (Figure S3, Supporting Information). To enhance detection performance, the incubation time of cells with the mixture of probes, hybridization time of the released barcodes on the DNA microarray, and HCR time were optimized to be 60, 90, and 30 min, respectively (Figure S4, Supporting Information).

Under the optimized conditions, the relationship between signal I and cell concentration was investigated by incubating the cells with probe mixture and performing the subsequent cleaving, capturing, HCR, and scanning steps. To obtain a suitable cell concentration range that could be used for glycan quantification and reduce the detection error for glycan number, different cell amounts were tested to investigate the relationship between the signal and cell concentration. For each type of barcode-lectin probes, the logarithm of I was found to be proportional to the logarithm of cell concentration (n) in the range from 5×10^2 to 5×10^4 cells/mL (Figure 6):

$$\log(I) = a \times \log(n) + b_2 \quad (2)$$

The slopes were the same as those for the corresponding coding DNA detection curves (eq 1) due to the same HCR efficiency, and the intercepts were +0.161, −0.671, −0.546, and −0.898 with the R values of 0.993, 0.990, 0.995, and 0.998 for A1-L-LCA, B1-L-SBA, C1-L-SNA, and D1-L-WGA, respectively. Thus, the average number (k) of glycan on each cell ($k = m/n$) could be calculated by eq 3:

$$k = 10^{\frac{b_2 - b_1}{a}} \quad (3)$$

From the intercepts and slopes, the average numbers of cell surface Man, GalNAc, Sia, and GlcNAc could be calculated to be 6.8×10^7, 3.8×10^7, 1.1×10^7, and 2.1×10^8 per cell, respectively (Figure 6c). The relative expression extent was in good agreement with the results from flow cytometric analysis using fluorescein lectins (Figure S5, Supporting Information), demonstrating the feasibility of the proposed method for simultaneous detection of multiple glycans on living cells. However, the flow cytometry-based strategies can only provide profiling information. Moreover, they require a large amount of sample for analysis and possess limited multiplex capability compared with the proposed method. The quantitative results were also verified by the consistence with other lectin-based strategies for Man[30−32] and chemoselective recognition-based strategy for Sia.[33] Compared with existed lectin array-based strategies,[34−36] the proposed strategy not only reserved the multiplexed detection capability but also achieved the quantification of multiple glycans on living cell surfaces.

CONCLUSIONS

A solution encoding strategy was developed for profiling and quantification of multiple glycans on whole living cell surfaces by combining it with a DNA microarray. Four types of barcode-lectin probes with distinct and specific glycan recognition capability were designed with DNA barcoding technology. These probes showed negligible DNA sequence cross-interference and could specifically bind to the corresponding glycans on cell surface. With an endonuclease cleaving step, the DNA barcodes could be released from cell surface, which were then captured by the DNA microarray to perform HCR-assisted DNA microarray fluorescence detection. The proposed method possessed the advantages of whole-surface accessibility, good resolution, enhanced sensitivity, and high throughput without any cell pretreatment or labeling. It could provide a powerful tool for investigation of glycan-related biological processes.

ASSOCIATED CONTENT

Supporting Information

Additional information as noted in the text. This material is available free of charge via the Internet at http://pubs.acs.org.

AUTHOR INFORMATION

Corresponding Author

*Phone/Fax: +86-25-83593593. E-mail: hxju@nju.edu.cn.

Author Contributions

†Y.C. and L.D. contributed equally to this work.

Notes

The authors declare no competing financial interest.

■ ACKNOWLEDGMENTS

We gratefully acknowledge National Basic Research Program (2010CB732400), National Natural Science Foundation of China (91213301, 21135002, 21322506, 21005037, 21121091), and PhD Fund for Young Teachers (20100091120034). We were supported by the Scientific Research Foundation of Graduate School of Nanjing University (2013CL01).

■ REFERENCES

(1) Varki, A. *Nature* **2007**, *446*, 1023−1029.
(2) Chen, I. J.; Chen, H. L.; Demetriou, M. *J. Biol. Chem.* **2007**, *282*, 35361−35372.
(3) Marth, J. D.; Grewal, P. K. *Nat. Rev. Immunol.* **2008**, *8*, 874−887.
(4) Ohtsubo, K.; Marth, J. D. *Cell* **2006**, *126*, 855−867.
(5) Pucic, M.; Pinto, S.; Novokmet, M.; Knezevic, A.; Gornik, O.; Polasek, O.; Vlahovicek, K.; Wang, W.; Rudd, P. M.; Wright, A. F.; Campbell, H.; Rudan, I.; Lauc, G. *Glycobiology* **2010**, *20*, 970−975.
(6) Dube, D. H.; Bertozzi, C. R. *Nat. Rev. Drug Discovery* **2005**, *4*, 477−488.
(7) Szymanski, C. M.; Michael, F. S.; Jarrell, H. C.; Li, J. J.; Gilbert, M.; Larocque, S.; Vinogradov, E.; Brisson, J. R. *J. Biol. Chem.* **2003**, *278*, 24509−24520.
(8) Hao, C.; Ding, L.; Zhang, X. J.; Ju, H. X. *Anal. Chem.* **2007**, *79*, 4442−4447.
(9) Fuster, M. M.; Esko, J. D. *Nat. Rev. Cancer* **2005**, *5*, 526−542.
(10) Pilobello, K. T.; Mahal, L. K. *Curr. Opin. Chem. Biol.* **2007**, *11*, 300−305.
(11) Rakus, J. F.; Mahal, L. K. *Annu. Rev. Anal. Chem.* **2011**, *4*, 367−392.
(12) Lis, H.; Sharon, N. *Chem. Rev.* **1998**, *98*, 637−674.
(13) Xie, M.; Hua, J.; Long, Y. M.; Zhang, Z. L.; Xie, H. Y.; Pang, D. W. *Biosens. Bioelectron.* **2009**, *24*, 1311−1317.
(14) Weis, W. I.; Drickamer, K. *Annu. Rev. Biochem.* **1996**, *65*, 441−473.
(15) Mitchell, P. *Nat. Biotechnol.* **2002**, *20*, 225−229.
(16) Ding, L.; Cheng, W.; Wang, X. J.; Ding, S. J.; Ju, H. X. *J. Am. Chem. Soc.* **2008**, *130*, 7224−7225.
(17) Pregibon, D. C.; Toner, M.; Doyle, P. S. *Science* **2007**, *315*, 1393−1396.
(18) Nam, J. M.; Thaxton, C. S.; Mirkin, C. A. *Science* **2003**, *301*, 1884−1886.
(19) Han, M.; Gao, X.; Su, J. Z.; Nie, S. *Nat. Biotechnol.* **2001**, *19*, 631−635.
(20) Nicewarner-Peña, S. R.; Freeman, R. G.; Reiss, B. D.; He, L.; Peña, D. J.; Walton, I. D.; Cromer, R.; Keating, C. D.; Natan, M. J. *Science* **2001**, *294*, 137−141.
(21) Service, R. F. *Science* **1995**, *270*, 577.
(22) Vaino, A. R.; Janda, K. D. *Proc. Natl. Acad. Sci. U.S.A.* **2000**, *97*, 7692−7696.
(23) Walt, D. R. *Science* **2005**, *308*, 217−219.
(24) Geiss, G. K.; Bumgarner, R. E.; Birditt, B.; Dahl, T.; Dowidar, N.; Dunaway, D. L.; Fell, H. P.; Ferree, S.; George, R. D.; Grogan, T.; James, J. J.; Maysuria, M.; Mitton, J. D.; Oliveri, P.; Osborn, J. L.; Peng, T.; Ratcliffe, A. L.; Webster, P. J.; Davidson, E. H.; Hood, L.; Dimitrov, K. *Nat. Biotechnol.* **2008**, *26*, 317−325.
(25) Venkatesan, B. M.; Bashir, R. *Nat. Nanotechnol* **2011**, *6*, 615−624.
(26) Severin, P. M. D.; Gaub, H. E. *Small* **2012**, *8*, 3269−3273.
(27) Seefeld, T. H.; Halpern, A. R.; Corn, R. M. *J. Am. Chem. Soc.* **2012**, *134*, 12358−12361.
(28) Schulze, H.; Barl, T.; Vase, H.; Baier, S.; Thomas, P.; Giraud, G.; Crain, J.; Bachmann, T. T. *Anal. Chem.* **2012**, *84*, 5080−5084.
(29) Dirks, R. M.; Pierce, N. A. *Proc. Natl. Acad. Sci. U.S.A.* **2004**, *101*, 15275−15278.
(30) Cheng, W.; Ding, L.; Lei, J. P.; Ding, S. J.; Ju, H. X. *Anal. Chem.* **2008**, *80*, 3867−3872.
(31) Ding, L.; Qian, R. C.; Xue, Y. D.; Cheng, W.; Ju, H. X. *Anal. Chem.* **2010**, *82*, 5804−5809.
(32) Han, E.; Ding, L.; Jin, S.; Ju, H. X. *Biosens. Bioelectron.* **2011**, *26*, 2500−2505.
(33) Chen, Y. L.; Ding, L.; Ju, H. X. *Chem. Commun.* **2013**, *49*, 862−864.
(34) Zheng, T.; Peelen, D.; Smith, L. M. *J. Am. Chem. Soc.* **2005**, *127*, 9982−9983.
(35) Chen, S. Y.; Zheng, T.; Shortreed, M. R.; Alexander, C.; Smith, L. M. *Anal. Chem.* **2007**, *79*, 5698−5702.
(36) Krishnamoorthy, L.; Bess, J. W., Jr.; Preston, A. B.; Nagashima, K.; Mahal, L. K. *Nat. Chem. Biol.* **2009**, *5*, 244−250.